CHINESE JOURNAL OF PHYSICS VOL. 42, NO. 5 OCTOBER 2004

First-Principles Study of the Electronic Structure of $BaTiO_3$ using Different Approximations

H. Salehi,[1] S. M. Hosseini,[2] and N. Shahtahmasebi[2]

[1]*Department of Physics, University of Shahid Chamran, Ahvaz, Iran*
[2]*Department of Physics, Ferdowsi University of Mashhad, Iran*

(Received February 10, 2003)

The electronic structure, energy band structure, and density of states (DOS) in paraelectric cubic crystal $BaTiO_3$ are studied by using the full potential-linearized augmented plane wave (FP-LAPW) method in the framework of density functional theory (DFT), with the generalized gradient approximation (GGA). The results show a direct band gap of 1.95 eV at the Γ point in the Brillouin zone. The calculated electronic structure, energy band structure, and density of states of $BaTiO_3$ are in good agreement with both the theoretical and experimental results. As in other perovskite ABO_3 ferroelectrics, there is hybridization between Ti-3d and O-2p, which is responsible for the ferroelectricity tendency.

PACS numbers: 71.15.Mb

I. INTRODUCTION

Ferroelectric and related materials, having the chemical formula ABO_3, have been the subject of extensive investigation, both because of their technical importance and their fundamental interest to physical and material sciences.

The ideal structure is a cubic perovskite, where the A and B cations are arranged on a simple cubic lattice, and the O ions lie on the face centers nearest to the B cations. The B cations are at the centers of the O octahedral, while the A cations lie at the larger 12-fold coordinated sites [1, 2]. The bonding between Ba and TiO_2 is mainly ionic, and the TiO_2 entity is bound covalently.

Barium titanate ($BaTiO_3$) is one of the most important ferroelectric oxides used in electronic applications. It has been widely used in electromechanical actuators and in sensor applications, as a major component of ceramic capacitor dielectrics, and in photo-galvanic devices [2–5]. It is also an important photo-refractive material used for applications in distortion correction and in combination with laser power. $BaTiO_3$ has three phase transitions, from cubic to tetragonal at 393 K, tetragonal to orthorhombic at 278 K, and orthorhombic to rhomohedral at 183 K [6, 7].

$BaTiO_3$ was the first advanced ceramic piezoelectric material, yet it is still often applied because of its chemical stability and high dielectric constant. An abrupt change of dielectric constant with temperature is the main difficulty with using the dielectric material. The ceramic type has positive temperature coefficient (PTC) properties. This is related to the grain properties of the ceramics which are optically opaque, while the single crystal is transparent. This material was the best piezoelectric ceramic until PZT ($PbZr_xTi_{1-x}O_3$

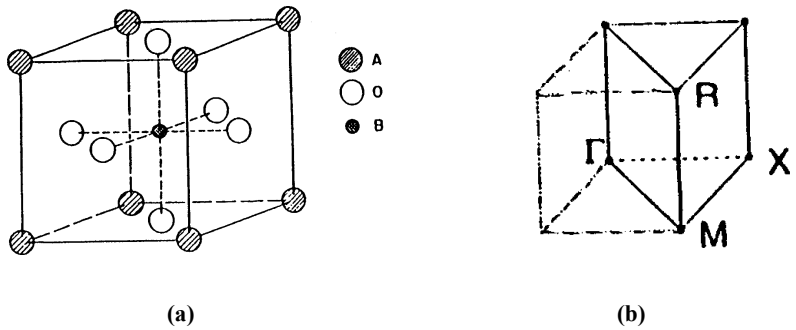

FIG. 1: (a) The cubic unit cell of $BaTiO_3$. (b) The Brillouin zone for cubic $BaTiO_3$.

with $x \simeq 0.52$) was discovered [3, 8].

Most studies that have been carried about electronic structure are experimental, only a few are theoretical [9]. In the present study, the electronic structure, density of states and the electronic density of cubic perovskite, $BaTiO_3$, in the paraelectric phase are calculated by the FP-LAPW method in the density functional theory (DFT) framework with the generalized gradient approximation (GGA) [10, 11].

The calculated results are compared with the experimental measurements; the results are in good agreement with the experimental results.

II. THE CALCULATION METHOD

The crystal structure of $BaTiO_3$ in the paraelectric phase has been studied experimentally using various techniques. The paraelectric phase is cubic and belongs to the space group pm(3)m. The cubic unit cell contains one molecule with the Ba sitting at the origin (0.0, 0.0, 0.0)a, the Ti at the body center (0.5, 0.5, 0.5)a and the three oxygen atoms at the three face centers (0.5, 0.5, 0.0)a, (0.0, 0.5, 0.5)a, and (0.5, 0.0, 0.5)a; the lattice constant is 7.57 a.u (1 a.u=0.529 Å) [6, 9]. Fig. 1(a) shows the unit cell and Fig. 1(b) shows the Brillouin zone of $BaTiO_3$ for this structure.

The electronic structure, total density of states (DOS), and electronic density in paraelectric cubic crystal $BaTiO_3$ are studied using the full potential-linearized augmented plane wave (FP-LAPW) method in the density functional theory (DFT) framework, with the generalized gradient approximation (GGA), by using the WIEN2k package. The calculations were done within the DFT with GGA for solving the Kohn-Sham equation [10, 11].

In the FP-LAPW method, space is divided into two regions, spherical "muffin-tins" around the nuclei, in which radial solutions of the Schrödinger equation and their energy derivatives are used as basis functions, and an "interstitial" region (I) between the muffin tins (MT), in which the basis set consists of plane waves. There is no pseudopotential approximation and core states are calculated self-consistently in the crystal potential.

Core states are treated fully relativistically, and valence and semi-core states are

treated semi-relativistically (i.e. ignoring spin-orbit coupling). In this method the valence and core states origin energies have been separated, and the −6 Ry energy bound separating between the valence electrons and the core states was chosen.

This method is a generalization of the LAPW method. The potential applied on the electron is in the most general state (without any especially figured assumption). The potential is similar to the wave function in the limit of a nucleus with too much variation and at large distances from the nucleus is quite smooth. In the two regions, MT and I, the potential is represented in different ways as follows:

$$V(r) = \begin{cases} \sum\limits_{k_n=0}^{k_n=max} V(\boldsymbol{k}_n) e^{i\boldsymbol{k}\cdot\boldsymbol{r}} & \text{(I)} \\ \sum\limits_{lm} V_{lm}(\boldsymbol{r}) Y_{lm}(\boldsymbol{r})\,. & \text{(MT)} \end{cases} \tag{1}$$

The potentials in the interstitial region have a Fourier expansion, and inside the muffin tin sphere they are expanded in terms of lattice harmonics. The lattice harmonic, Y_{lm}, is made up of a combination of a spherical harmonic, y_{lm}, and a lattice point group. The implementation of Y_{lm}, in state y_{lm} needs less space for data storage, and speeds up the calculation. The basis functions for expanding the electronic wave functions are:

$$\varphi(k_n, r) = \begin{cases} \dfrac{1}{\sqrt{\Omega}} e^{i\boldsymbol{k}_n\cdot\boldsymbol{r}} & \text{(I)} \\ \sum\limits_{l=0}^{\infty} \sum\limits_{m=-1}^{+1} \left[A_{lm}(\boldsymbol{k}_n) u_l(r, E_l) + B_{lm}(\boldsymbol{k}_n) u_l^0(r, E_l)\right] Y_{lm}(r)\,, & \text{(MT)} \end{cases} \tag{2}$$

where $u_l(r, E_l)$ is the (at the origin) regular solution of the radial Schrödinger equation for energy constant E_l inside the MT sphere, and $u_l^0(r, E_l) = \frac{\partial u_l(r,E_l)}{\partial E}|_{E=E_l}$ is the energy E derivative of U_l evaluated at some energy E_l, Ω is the cell volume, and $\boldsymbol{k}_n = \boldsymbol{k} + \boldsymbol{g}_n$, where $\boldsymbol{g}_n$ is the reciprocal lattice vectors and $\boldsymbol{k}$ is the wave vector inside the first Brillouin zone.

This method does not need to have E_l as a Kohn-Sham energy eigenvalue but E_l is a constant value, if E_l is chosen reasonably. In this case the results are more accurate and the volume of calculation is decreased.

III. RESULTS

III-1. Electronic Structure

For calculating the lattice constant theoretically, the base-state energy of $BaTiO_3$ is calculated for different volumes around the balance volume. The changes of energy in the volumes are given by the Murnaghan equation of state. The total energy as a function of the volume for cubic $BaTiO_3$ is shown in Fig. 2.

The results show that the GGA condensation module is much closer to the experimental and the theoretical volumes. In the LDA (Local Density Approximation), however, there are noticeable differences between the experimental and theoretical volumes. The lattice constant calculated by the FP-LAPW method or the GGA96 approximation is closer to the experimental values. The difference may be related to virtual pressure.

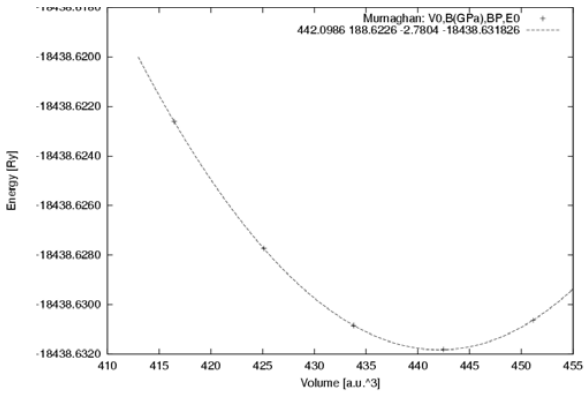

FIG. 2: Total energy as a function of the volume for cubic $BaTiO_3$

TABLE I: Structure parameters calculated in this work compared with other results for cubic barium titanate.

	FP-LAPW GGA96	FP-LAPW GGA91	FP-LAPW LDA	Experimental [2,11,13]	Theoretical LDA[14]	Experimental [15,16]	Pseudo-potential[17]
a(au)	7.5	7.61	7.44	7.57	7.45	7.56	7.456
B(Gpa)	188.6226	184.6277	145.7770	173	195	-	-
B^l(Gpa)	-2.7804	-1.9708	-1.9143	-	-	-	-
k(m^2/N)	5.3×10^{-14}	5.4×10^{-14}	6.9×10^{-14}	6.4×10^{-14}	65.1×10^{-14}	-	-
E_0(Ry)	-18438.63	-18441.64	-18419.89	-	-	-	-

The distances between the nearest atoms are shown in Table II for cubic barium titanate. These lengths, for the experimental and theoretical results, are equal, and do not depend on the exchange correlation potentials.

The effective charges on the three Ba, Ti, and O atoms are shown in Table III and are very close to the value of the ionic charge. These charges for both the experimental and theoretical results are also equal. This gives the $BaTiO_3$ ionic formula $Ba^{+1.73}Ti^{+2.04}[O^{-1.72}]_3$.

TABLE II: A comparison of the nearest distance between atoms for cubic barium titanate.

	FP-LAPW GGA96 with Theoretical Constant	FP-LAPW GGA96 with experimental Constant	FP-LAPW GGA91 with Theoretical Constant	FP-LAPW GGA91 with experimental Constant	FP-LAPW LSDA with Theoretical Constant	FP-LAPW LSDA with experimental Constant	Experimental [2]
Ba-O	5.3033	5.35280	5.3033	5.35280	5.3033	5.35280	3.3548
Ti-O	3.75	3.785	3.75	3.785	3.75	3.785	3.791

TABLE III: Effective charge calculated in this work compared with other results for cubic barium titanate.

	FP-LAPW GGA96 with Theoretical constant	FP-LAPW GGA96 with experimental constant	FP-LAPW GGA91 with Theoretical constant	FP-LAPW GGA91 with experimental constant	FP-LAPW LDA with Theoretical constant	FP-LAPW LDA with experimental constant	TB-LMTO	Formula
Ba	1.7287	1.7282	1.7294	1.7277	1.7290	1.7287	-1.5	+2
Ti	2.0408	2.0378	2.0407	2.0341	2.0411	2.0345	1.44	+4
O	1.7231	1.7223	1.7228	1.7203	1.7141	1.7116	0.06	-2

III-2. Band Structure

The crystal structure of $BaTiO_3$ in the paraelectric phase has been studied experimentally using various techniques [6, 7, 9]. In this method 400 k-points were used and a convergence parameter, $Rk_{max} = 7$, was chosen. The convergence was stable in terms of energy. The calculated energy-band structure for cubic phases $BaTiO_3$ is shown in Fig. 3. The energy scale is in eV, and the origin of energy was arbitrarily set to be at the maximum of the valence band. The results indicate that there is a large dispersion of the bands. Nine valence bands are derived from the oxygen 2p orbital which are separated by a direct gap of 1.95 eV (at the Γ point) from the transition-metal d-derived (Ti) conduction band. This gap is somewhat lower than the experimental band gap of 3eV for $BaTiO_3$ [2, 12]. The origin of this discrepancy may be the GGA. The nine valence bands at the Γ point are the three triply degenerate levels (Γ_{15}, Γ_{25}, and Γ_{15}), separated by energies of 1.15 eV ($\Gamma_{25} - \Gamma_{15}$) and 1.1 eV ($\Gamma_{15} - \Gamma_{25}$). The crystal field and the electrostatic interaction between the oxygen 2p orbital produces this splitting.

In the conduction band the triply ($\Gamma_{25'}$) and doubly (Γ_{12}) degenerate levels represent t_{2g} and e_g states of the titanate 3d orbital are separated by an energy of 2.1 eV. A visual comparison of our band structure results with the result of reference [1, 2] on $BaTiO_3$ shows a direct band gap at the Γ point, using the pseudopotential method equal by the FP-LAPW method. A comparison between this result and reference [9] for $BaTiO_3$ shows almost no discernible difference, except that they obtained a direct band gap of 1.2 eV at the Γ point using the TB-LMTO method.

The result for the band gap calculated by this method and others are summarized in Table IV. The band gap calculated by this method, with the GGA approximation, is 1.8 eV. The band gap is smaller than the experimental result of 3 eV, probably due to a discrepancy in the GGA method. If we add a correction factor to this band gap, the results are found to be in excellent agreement with the experimental data.

III-3. Density of states and electronic density of states

The calculated valence bands below the Fermi energy agree well with other first-principle studies [2, 6, 7]. The electronic structure shown in Fig. 3 was calculated using

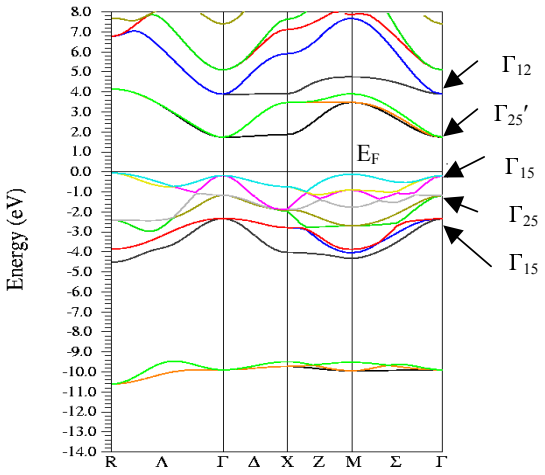

FIG. 3: The calculated electronic band structure for cubic $BaTiO_3$. The zero of the energy was set at the top of the valence band.

TABLE IV: The results for the band gap calculated by this method and others.

	FP-LAPW GGA96 with Theoretical Constant	FP-LAPW GGA96 with experimental Constant	FP-LAPW GGA91 with Theoretical Constant	FP-LAPW GGA91 with experimental Constant	FP-LAPW LDA with Theoretical Constant	FP-LAPW LDA with experimental Constant
Typical Gap	Γ	Γ	Γ	Γ	Γ	Γ
Band Gap	1.85eV	1.95eV	1.9eV	1.95eV	1.8eV	1.85eV
Difference with experimental(%)	3.83	35	36.7	35	40	38.3
$\Gamma_{15}-\Gamma_{25}$	1.1eV	1.15eV	1.1eV	1.15eV	1.15eV	1.15eV
$\Gamma_{15}-\Gamma_{25}$	1.05eV	1.1eV	1.05eV	2eV	1.09eV	1eV
$\Gamma_{15}-\Gamma_{25}$	2.15eV	2.1eV	2.15eV	2.1eV	2.4eV	2.2eV

	TB-LMTO [9]	Pseudopotentail [18]	Experimental [2,5]
Typical Gap	Γ	Γ	Γ
Band Gap	1.2eV	1.8eV	3eV
Difference with experimental(%)	60	40	0
$\Gamma_{15}-\Gamma_{25}$	1.14eV	-	-
$\Gamma_{15}-\Gamma_{25}$	1.09eV	-	-
$\Gamma_{15}-\Gamma_{25}$	2.15eV	-	-

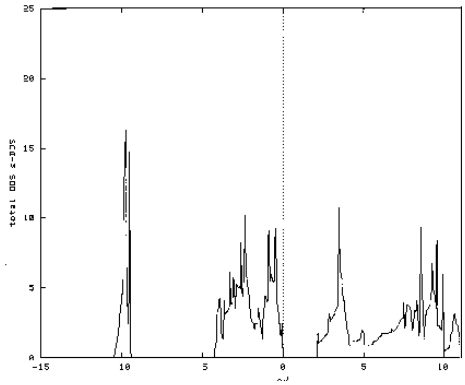

FIG. 4: The density of states (DOS) for paraelectric cubic $BaTiO_3$

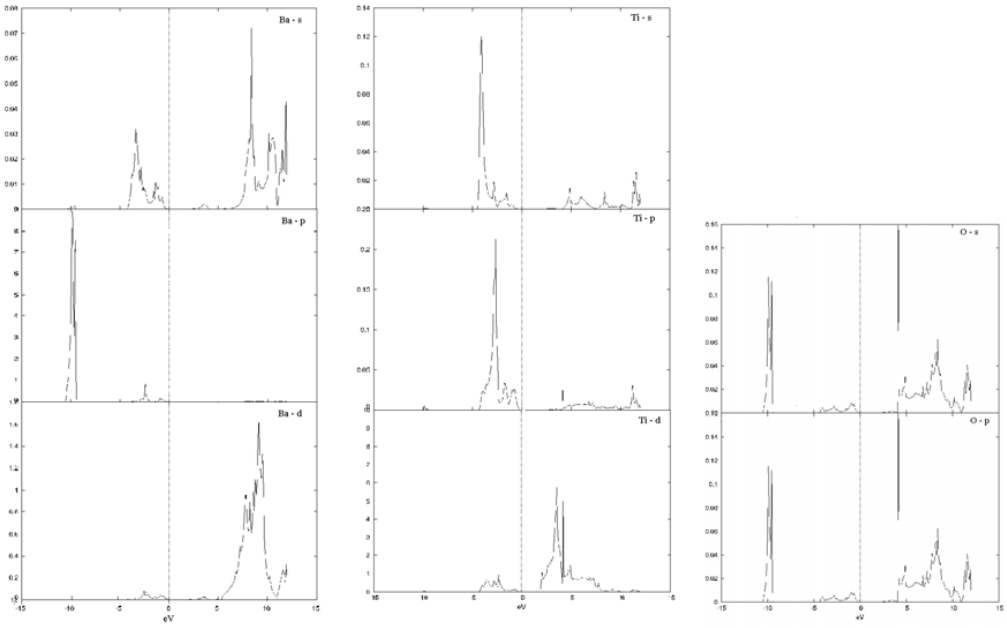

FIG. 5: The density of states (DOS) for paraelectric cubic $BaTiO_3$

the lattice constant 7.57 a.u. In Fig. 3 the zero of the energy scale shows the position of the Fermi level. The Ti-3d contribution is zero at the maximum of the valence band, but rises strongly with increasing binding energy. Conversely, the oxygen 2p contribution rises from zero at the minimum of the conduction band with increasing energy. This reflects the Ti-3d–O-2p covalency. The electron distribution in an energy spectrum is described by the density of states (DOS) and can be measured in photoemission experiments. The total DOS spectrum of cubic $BaTiO_3$ is shown in Fig. 4. The valence and conduction band edges near the Fermi energy are quite sharp.

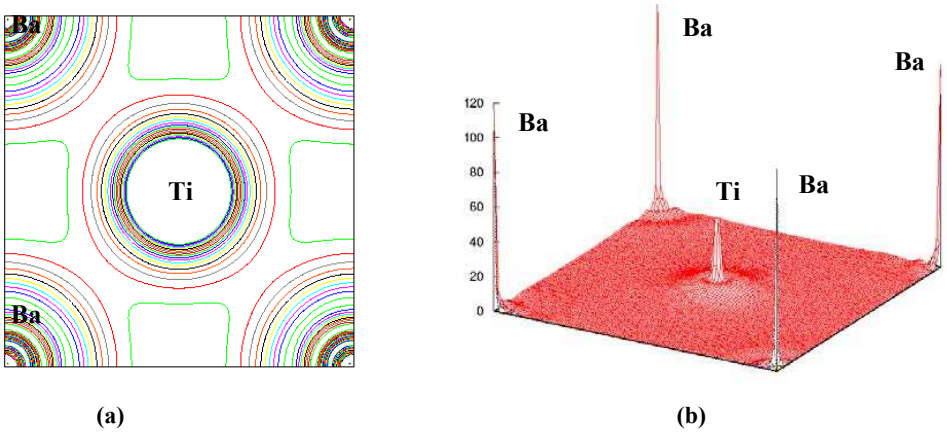

FIG. 6: Electron density distribution for $BaTiO_3$: (a) in the (100) plane and (b) in three dimension.

The partial density of states (PDOS) of the Ba, Ti, and O atoms are shown in Fig. 5. The low-energy peak around 17 to 15.5 eV is a contribution mainly from the O-2s states, with a small component from the Ti-p and O-p orbitals. The DOS peak at around 10 eV mainly represents the contribution of the Ba 5p states, which are weakly hybridized with the O-s and O-p states. The valence states, from 4.7 eV up to the Fermi energy, are dominated by the O-2p states and strongly hybridized with the Ti-3d state. It should be pointed out that the PDOS spectrum in Fig. 5 includes one Ba atom, one Ti atom, and three O atoms. Therefore the height of the O-2p DOS peak is much higher than that of the Ti-3d states.

A quick estimate suggests that there is only a very weak hybridization of the Ba-p state with the O-2p state, but there is a very strong hybridization between the Ti-3p and O-2p state in the valence band. This means that this system does not quite have an ionic bond, but it has a rather large covalency. This is shown in Fig. 6 for the (100) plane and in Fig. 7 for the (110) plane. The electron density distribution indicates that the bond between Ba and TiO_2 is ionic, while that between the Ti and O is covalent.

IV. CONCLUSIONS

We have made a detailed investigation of the electronic structure, band structure, and DOS of paraelectric $BaTiO_3$ in the cubic phase, using the FP-LAPW method. The effective charge on the three Ba, Ti, and O atoms, are very close to the value of the ionic charge. This gives the ionic formula for $BaTiO_3$ to be $Ba^{+1.73}Ti^{+2.04}[O^{-1.72}]_3$. This means there is slightly more charge transfer from the Ba to the O atom as a result of the relative position shift and the small volume effect. The calculations show that the fundamental gap in $BaTiO_3$ is direct at the Γ point. The band gap calculated by this method with the GGA approximation is 1.95 eV. This band gap is smaller than the experimental result of 3 eV,

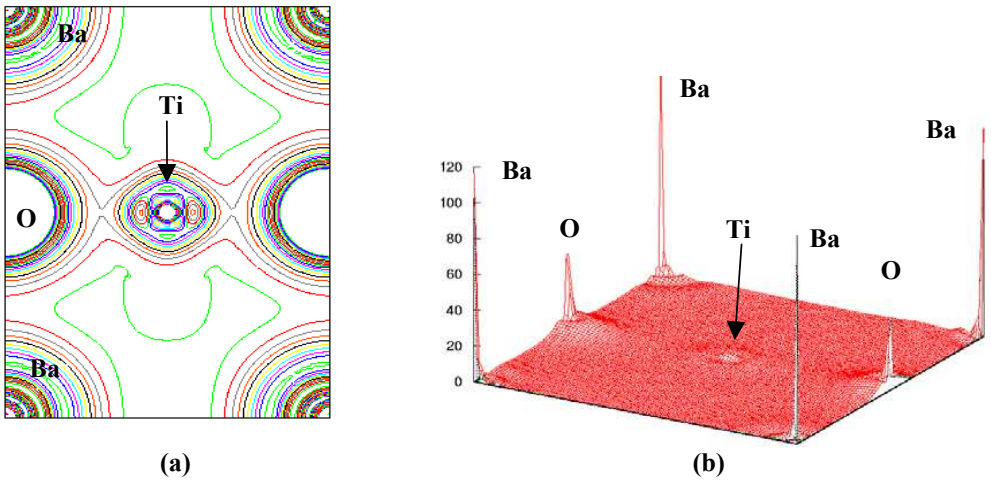

FIG. 7: Electron density distribution for $BaTiO_3$: (a) in the (110) plane and (b) in three dimension.

probably due to a discrepancy in the GGA method. If we add a correction factor to this band gap, the results are found to be in excellent agreement with the experimental data.

The total DOS obtained by this method shows a very weak hybridization of the Ba-p state with the O-2p state, but there is a very strong hybridization between the Ti-3p and O-2p state in the valence band. This means that this system does not quite have an ionic bond, but it has a rather large covalency.

References

[1] D. Bagayoko, G. L. Zhao, J. D. Fan, and J. T. Wang, Proc. Louisiana Acad. Sci. **60**, 43 (1997).
[2] D. Bagayoko, G. L. Zhao, J. D. Fan, and J. T. Wang, J. Phys. Condensed Matter **10**, 5645 (1998).
[3] A. J. Moulson, J.M. Herbert, *Electroceramics*, (Chapman and Hall, 1990).
[4] M. Gardana, Phys. Rev. **140**, A651 (1965).
[5] R. T. Mara, G. B. B. Sutherland, and H. V. Tyrell, Phys. Rev. **96**, 801 (1954).
[6] R. E. Cohen and H. Krakuer, Ferroelectrics **136**, 65 (1992).
[7] R. E. Cohen and H. Krakuer, Phys. Rev. B **42**, 6416 (1990).
[8] W. D. Kingery, H. K. Bowen, and D. R. Uhlman, *An Introduction to Ceramics*, (John Wiley & Sons Inc., 1975).
[9] S. Saha, T. P. Sinha, and A. Mookerjee, Phys. Rev. B **62**, 8828 (2000).
[10] J. P. Perdew, J. A. Chevary *et al*, Phys. Rev. B **46**, 6671 (1992).
[11] J. P. Perdew, Physical. B **172**, 1 (1991).
[12] S. H. Wemple, Phys. Rev. B **2**, 2679 (1970).
[13] M. Kitamura and H. Chen, Ferroelectrics **210**, 13 (1998).
[14] D. D. Koelling, Phys. Rev. B **2**, 290 (1970).
[15] M. Peterson, F.Wanger, L. Hufnagel, M. Scheffler, and P. Blaha, Computer Physics Communication **126**, 294 (2000).

[16] D. C. Langreth and M. J. Mehl, Phys. Rev. B **28**, 1809 (1983).
[17] D. Balzar, H. Ledbetter, P. W. Stephens, E. T. Park, and J. L. Routbort, Phys. Rev. B **59**, 5 (1999).
[18] R. D. King-Smith and D. Vanderbilt, Phys. Rev. B **49**, 5828 (1994).
[19] F. M. Michel-Calendini and G. Mesnard, J. Phys. C. Solid State Phys. **6**, 1709 (1973).
[20] K. Schwarz, P. Blaha, and G. K. H. Madsen, Computer Physics Communications, 1 (2002).
[21] M. Kitamura and H. Chen, Ferroelectrics **206-207**, 55 (1998).
[22] P. Blaha and K. Schwarz, WIEN2k, (Vienna University of Technology, Austria, 2002).
[23] P. H. Ghosez, X. Gonze, and J. P. Michenaud, Ferroelectrics **153**, 91 (1994).
[24] S. H. Wei and H. Krakauer, Phys. Rev. Lett. **55**, 1200 (1985).